

CHEMISTRY

AN ASIAN JOURNAL

www.chemasianj.org

Accepted Article

Title: Suspending Ion Electrocatalysts in Charged Metal-Organic Frameworks to Improve the Conductivity and Selectivity in Electroorganic Synthesis

Authors: Chuan-De Wu, Wei-Wei Guo, Chi Zhang, Ji-Jie Ye, Zi-Kun Liu, and Kai Chen

This manuscript has been accepted after peer review and appears as an Accepted Article online prior to editing, proofing, and formal publication of the final Version of Record (VoR). This work is currently citable by using the Digital Object Identifier (DOI) given below. The VoR will be published online in Early View as soon as possible and may be different to this Accepted Article as a result of editing. Readers should obtain the VoR from the journal website shown below when it is published to ensure accuracy of information. The authors are responsible for the content of this Accepted Article.

To be cited as: *Chem. Asian J.* 10.1002/asia.201900640

Link to VoR: <http://dx.doi.org/10.1002/asia.201900640>

A Journal of



A sister journal of *Angewandte Chemie*
and *Chemistry – A European Journal*

WILEY-VCH

Suspending Ion Electrocatalysts in Charged Metal-Organic Frameworks to Improve the Conductivity and Selectivity in Electroorganic Synthesis

Wei-Wei Guo,^[a] Chi Zhang,^[a] Ji-Jie Ye,^[a] Zi-Kun Liu,^[a] Kai Chen,^[a] and Chuan-De Wu^{*[a]}

Dedicated to Professor Jin-Shun Huang on the occasion of his 80th birthday

Abstract: Electroorganic synthesis is an environmentally friendly alternative to traditional synthetic methods; however, the application of this strategy is heavily hindered by low product selectivity. Metal-organic frameworks (MOFs) exhibit high selectivity in numerous catalytic reactions; however, poor conductivity heavily limited the application of MOFs in electroorganic synthesis. To realize electrocatalytic application of MOFs in selective electroorganic synthesis, we report a practically applicable strategy by suspending ion electrocatalysts in charged MOFs, which could markedly improve product selectivity in electroorganic synthesis. In electrocatalytic oxidative self-coupling of benzylamine experiments, the imine product selectivity is markedly improved from 61.3 to 94.9%, when the MOF-based electrocatalyst is used instead of the corresponding homogeneous electrocatalyst under the identical conditions. Therefore, this work opens a new window to improve the product selectivity in electroorganic synthesis.

Introduction

Organic electrochemistry has been emerged as an environmentally friendly, atom-economic and sustainable alternative to traditional synthetic methods, thanks to the use of clean redox power in place of stoichiometric amount of oxidants or reductants.^[1-3] The reactivity of electrochemical reactions is systematically tunable by changing the applied potentials, which makes certain complex molecules easily accessed under mild conditions.^[4] Over the past decade, electrochemistry has been an effective strategy for the synthesis of high value-added chemicals by forming C-C,^[5,6] C-N,^[7,8] C-O,^[9-11] C-S,^[12-14] C-P,^[15] and C-Hal bonds.^[16,17] Some significant redox reactions were also easily realized by electrochemical reactions, such as ammonia synthesis^[18-20] and CO₂ reduction.^[21,22] However, there remain some issues that hinder the practical applications of this strategy in organic synthesis, including low catalyst turnovers, low product selectivity, and low stability and conductivity of working electrodes.^[2,3,23]

Metal-organic frameworks (MOFs) are a class of porous

materials constructed from multidentate organic ligands and metal ions/clusters, featuring high porosity, high surface areas, and tunable pore sizes and shapes.^[24-26] MOFs have been emerged as a powerful platform to integrate variety of functional molecular entities in the pores/matrices for applications in different fields.^[27-43] The tunable pore nature and constituents of MOFs endow systematically introduce different redox-active and auxiliary centers to tune the catalytic properties for highly efficient and selective catalysis.^[32-43] MOFs have also been appeared in electrocatalysis, such as oxygen reduction reaction,^[44,45] hydrogen evolution reaction,^[46,47] electroreduction of CO₂^[48,49] and electrooxidation of ethanol.^[50] However, the inherent low conductivity of most MOFs heavily deteriorated their electrocatalytic properties, especially in electroorganic synthesis.

Several approaches, trying to improve the electrical conductivity of MOFs, have been developed in recent years.^[51,52] One strategy was to construct two-dimensional (2D) MOFs by forming planar π -d conjugated sheets, which exhibit comparable conductivity with graphite.^[53] However, this strategy could not be applied to three-dimensional (3D) MOFs, because their building moieties are uniformly isolated in the 3D pore matrices. Another attempt was to impregnate graphene and carbon nanotubes into MOFs to generate composite conductive materials.^[54] However, this strategy could not fundamentally solve the inherent low conductivity issue of MOFs. Attempts were also made to improve the electrical conductivity of MOFs by using softer sulfur-based organic linkers to combine with selected metal ions.^[55] The application of this method is heavily hindered by the complex synthetic procedures and the scope of MOFs. An alternative approach was to engineer long-range delocalization through installation of closely spaced mixed-valence functionalities to promote inter-valence charge transfer.^[56] It is unfortunate that direct synthesis of mixed-valence MOFs remains a challenge.

Ionic conduction has been realized widespread applications in the electrolytes of batteries and fuel cells, gas sensors and biomaterials chemistry.^[57] It has been demonstrated that introducing ionic liquids into MOFs would result in highly conductive materials.^[58] We have shown that confining metal cations in the anionic pores of ionic MOFs would endow the catalytic sites freely mobile, which are easily accessed to reactant molecules in heterogeneous catalysis.^[59,60] If suspended ion catalysts (SICs) are used as heterogeneous electrocatalysts, the freely mobile ionic active sites should be easily reached to working electrodes induced by electric field. By tuning the pore sizes, shapes and properties of ionic MOFs, the electrochemical selectivity in electroorganic synthesis would be

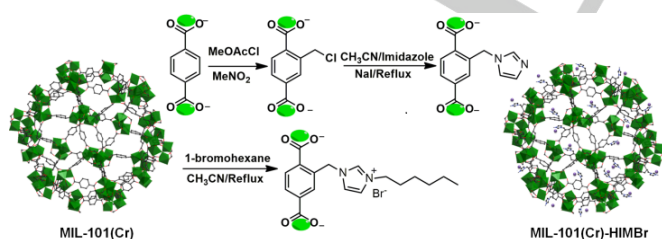
[a] Wei-Wei Guo, Chi Zhang, Ji-Jie Ye, Zi-Kun Liu, Kai Chen, and Prof. Dr. Chuan-De Wu
State Key Laboratory of Silicon Materials
Department of Chemistry
Zhejiang University
Hangzhou, 310027, P. R. China
E-mail: cdwu@zju.edu.cn

Supporting information for this article is given via a link at the end of the document.

systematically improved, controlled by the special pore microenvironment. When a suspended ion electrocatalyst TEMPO-SO₃@MIL-101(Cr)-HIM (HIM = hexane imidazolium), consisting of cationic framework MIL-101(Cr)-HIM and suspended anionic active sites TEMPO-SO₃⁻ in the charged pores, was immobilized on working electrode, it demonstrates high catalytic efficiency and selectivity in electro-oxidative self-coupling of benzylamines, which is much superior to the corresponding homogenous molecular catalyst.

Results and Discussion

The pristine MOF MIL-101(Cr) was synthesized according to the literature, which was further reacted with aluminium chloride and methoxyacetyl chloride in nitromethane to generate chloromethylated product MIL-101(Cr)-CH₂Cl (Scheme 1).^[61-63] MIL-101(Cr)-HIMBr was synthesized by reaction of MIL-101(Cr)-CH₂Cl with imidazole, and subsequent with 1-bromohexane.^[64,65] The structural identity of as-synthesized MIL-101(Cr) and post-modified MIL-101(Cr)-HIMBr was characterized by monitoring the PXRD patterns (Figure S1). All samples display good crystallinity and the diffraction peaks match well with those of the simulated, which proved the same structural identity of MIL-101(Cr) and MIL-101(Cr)-HIMBr. In the FT-IR spectrum of MIL-101(Cr)-HIMBr, the peaks at 1660, 1330, 1250 and 1104 cm⁻¹ are attributed to the stretching vibrations of imidazolium moieties (Figure S2).^[63] The band at 1584 cm⁻¹ corresponds to the stretching vibration of C=N bonds in imidazolium, which confirmed successfully anchoring of imidazolium moieties on the framework of MIL-101(Cr)-HIMBr. Additionally, the bands at 2929 and 3135 cm⁻¹ are derived from the stretching mode of aromatic C-H and the aliphatic C-H on imidazolium, respectively, which are other evidences to prove the existence of imidazolium moieties in MIL-101(Cr)-HIMBr. SEM and TEM images show that the octahedral morphology of MIL-101(Cr) is well reserved for the post-modified MIL-101(Cr)-HIMBr (Figure 1a and 1b). Elemental mapping images show that Br and N elements are well distributed in the post-modified crystalline solid MIL-101(Cr)-HIMBr (Figure 1c and 1d).



Scheme 1. Schematic representation of the synthetic procedures for MIL-101(Cr)-HIMBr.

N₂ physical adsorption-desorption isotherms of MIL-101(Cr) and MIL-101(Cr)-HIMBr are the typical type I N₂ sorption isotherms, featuring characteristics of microporous materials

(Figure 1e). The BET surface area of post-modified MIL-101(Cr)-HIMBr is of 2163.71 m²/g, which is slightly smaller than that of the pristine MIL-101(Cr) (2526.74 m²/g). DFT analysis of the pore size distributions showed that the pore sizes of MIL-101(Cr)-HIMBr are also slightly smaller than those of the pristine MIL-101(Cr) (Figure 1f and Table S1). These results should be ascribed to grafting of imidazolium moieties on the framework of MIL-101(Cr)-HIMBr. It is worth noting that there remains very large pore space in MIL-101(Cr)-HIMBr, which is ready for subsequent introduction of anionic electrocatalysts inside the cationic pores through ion exchange.

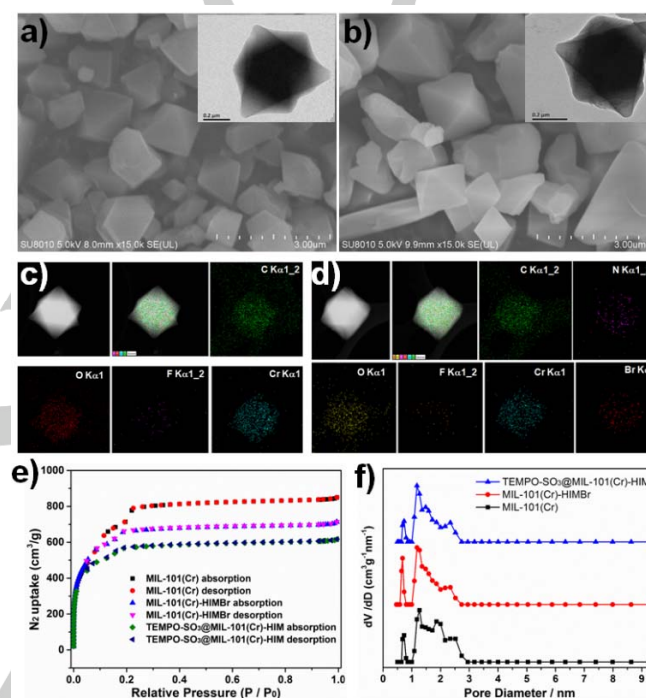


Figure 1. SEM and TEM (insert) images (a and b), and elemental mapping images (c and d) for MIL-101(Cr) (left column) and MIL-101(Cr)-HIMBr (right column), (e) N₂ physical adsorption-desorption isotherms of MIL-101(Cr), MIL-101(Cr)-HIMBr and TEMPO-SO₃@MIL-101(Cr)-HIM, and (f) their pore size distributions, calculated by DFT method.

Electrochemical impedance spectroscopy (EIS) measurements were conducted to investigate the interfacial electron transfer capability between cationic MIL-101(Cr)-HIMBr and electrode surface by using the redox probe [Fe(CN)₆]^{3-/4-} (Figure 2a). The working electrode was prepared by pipetting a suspension of MIL-101(Cr)-HIMBr in PVDF NMP and H₂O solution onto a glassy carbon electrode. The EIS of MIL-101(Cr)-HIMBr exhibits a high-frequency semicircle and a low-frequency tail, which is the typical impedance plot for ionic materials. The semicircle is given by the bulk electrical properties of MIL-101(Cr)-HIMBr relating to the electron transfer limited process, and the tail corresponds to the diffusion at the interface between electrode and electrolyte.^[66] Compared with that for the pristine MIL-101(Cr) (166 Ω), the semicircle diameter (108 Ω), equal to

the electron transfer resistance (R_{et}) in the Nyquist diagram, in the high-frequency region for MIL-101(Cr)-HIMBr is evidently reduced. The decrease in the diameter of the semicircle indicates the decrease in the resistance of electron transfer of $[\text{Fe}(\text{CN})_6]^{3-/4-}$ redox couple between the solution and the electrode, demonstrating that ionic MIL-101(Cr)-HIMBr formed high electron conduction pathways between the electrode and electrolyte. These results could be attributed to the electrostatic attraction between the positively charged framework and $[\text{Fe}(\text{CN})_6]^{3-/4-}$ anions, which could accelerate the anion transfer and improve the diffusion of $[\text{Fe}(\text{CN})_6]^{3-/4-}$ toward the electrode surface for fast electron transfer. Compared with the MIL-101(Cr) coated electrode, the MIL-101(Cr)-HIMBr coated electrode presents larger anodic and cathodic currents in the cyclic voltammogram (CV) curve, indicating that cooperation of ionic MIL-101(Cr)-HIMBr could accelerate electron transfer, which is in accordance with the EIS results (Figure 2b). The markedly improved electrical conductivity and interfacial charge transfer capability of ionic MIL-101(Cr)-HIMBr would be able to improve the electrocatalytic efficiency in electroorganic synthesis.

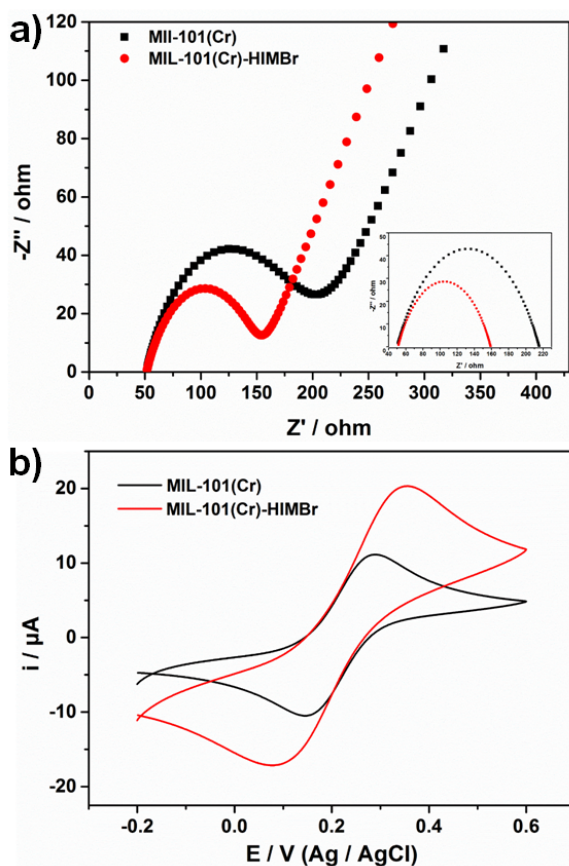


Figure 2. (a) Electrochemical impedance spectra of MIL-101(Cr) and MIL-101(Cr)-HIMBr in 0.1 M KCl solution containing 5 mM $[\text{Fe}(\text{CN})_6]^{3-/4-}$ at room temperature. (b) Cyclic voltammograms of MIL-101(Cr) and MIL-101(Cr)-HIMBr in 5 mM $[\text{Fe}(\text{CN})_6]^{3-/4-}$ in the presence of 0.1 M KCl supporting electrolyte at a scan rate of 20 mV s^{-1} with platinum wire as the counter electrode and Ag/AgCl as the reference electrode.

We have demonstrated that suspending redox-active metal cations inside the anionic pores of ionic MOFs would result in SICs, in which the active sites are freely mobile to significantly improve the catalytic efficiency.^[59,60] The endogenous Br^- anions inside the cationic pores of MIL-101(Cr)-HIMBr should be systematically replaceable with different anionic redox-active moieties to develop electrochemical SICs by ion exchange. Because the size of TEMPO-SO_3^- is much smaller than the pore window dimensions of MIL-101(Cr)-HIMBr, the anionic catalyst should easily diffuse into the pore space by ion exchange. Treatment of MIL-101(Cr)-HIMBr with BF_4^- and subsequent with TEMPO-SO_3^- resulted in a SIC material $\text{TEMPO-SO}_3@$ MIL-101(Cr)-HIM, in which the extra-framework Br^- anions were almost fully exchanged by TEMPO-SO_3^- anions as confirmed by EDX spectroscopy, elemental mapping images and HPLC analysis (Figures S3-S6 and Table S2). Because the coordination ability of sulfonate is very weak, anionic TEMPO-SO_3^- should be freely mobile but not able to leach out of the cationic pores confined by the strong electrostatic interaction between cationic host and anionic guests. PXRD patterns showed that the fundamental structure of $\text{TEMPO-SO}_3@$ MIL-101(Cr)-HIM was retained during ion exchange process (Figure S8). FT-IR spectrum of $\text{TEMPO-SO}_3@$ MIL-101(Cr)-HIM shows the typical stretching vibration bands at 1220 and 1197 cm^{-1} for S=O bond in TEMPO-SO_3^- , which further confirmed encapsulation of TEMPO-SO_3^- in the cationic pores (Figure S9).^[67] N_2 physical adsorption-desorption isotherms of an activated solid sample of $\text{TEMPO-SO}_3@$ MIL-101(Cr)-HIM show that it takes up 730 $\text{cm}^3 \text{g}^{-1}$ N_2 at 77 K and 1 bar, resulting in a BET surface area of 1791.3 $\text{m}^2 \text{g}^{-1}$ with the micropore widths in the range of 0.7-2.3 nm (Figure 1e and 1f). Compared with those of the pristine MIL-101(Cr)-HIMBr, the BET surface area and pore sizes are slightly decreased due to encapsulation of TEMPO-SO_3^- anions inside the cationic pores.

Imines and their derivatives are a class of highly reactive and important intermediates for preparation of heterocyclic chemicals, pharmaceuticals and fine chemicals.^[68] Imines were traditionally synthesized by condensation of amines and carbonyl compounds. However, this approach requires dehydrating agents and activated aldehydes catalyzed by Lewis acids, which is not an environmentally friendly approach.^[69] As an alternative strategy, electrosynthesis is a simple and green synthetic approach, which does not require additional contaminative agents. We therefore selected electro-oxidative self-coupling of benzylamine as a model reaction to evaluate the mobility, accessibility, stability and activity of suspended ion electrocatalyst TEMPO-SO_3^- in $\text{TEMPO-SO}_3@$ MIL-101(Cr)-HIM.

The electrochemical behaviors of $\text{TEMPO-SO}_3@$ MIL-101(Cr)-HIM were investigated by monitoring the CV curves at room temperature in acetonitrile containing 0.1 M Bu_4NBF_4 supporting electrolyte. The potentials reported herein are referenced to Ag/AgCl (in 3 M KCl) reference electrode, which is 0.194 V vs. standard hydrogen electrode (SHE). As shown in Figure 3 (curve a), $\text{TEMPO-SO}_3@$ MIL-101(Cr)-HIM exhibits a reversible oxidation wave at +0.858 V and a cathodic peak at +0.830 V. When benzylamine was added into the solution, the oxidation peak current increased dramatically, while the

corresponding reduction peak current decreased (curve b). The obvious increase of electron current indicates that electro-redox catalysis occurred between TEMPO-SO₃⁻ and benzylamine under the conditions.

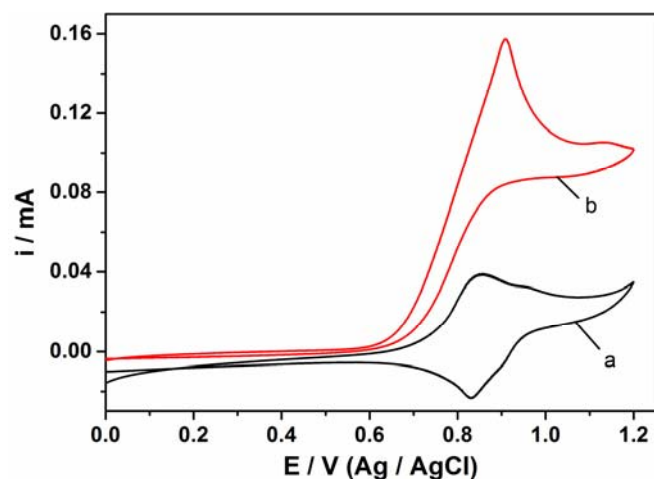


Figure 3. Cyclic voltammograms of TEMPO-SO₃@MIL-101(Cr)-HIM in Bu₄NBF₄/CH₃CN solution (curve a) and in the presence of benzylamine (curve b) at a scan rate of 20 mV s⁻¹ on the glassy carbon working electrode with platinum wire as the counter electrode and Ag/AgCl as the reference electrode.

Electrocatalysis was conducted in an undivided cell with working electrode as the anode, platinum wire as the cathode, Bu₄NBF₄ as the electrolyte and CH₃CN as the solvent. The working electrode was prepared by pipetting a suspension of TEMPO-SO₃@MIL-101(Cr)-HIM in PVDF NMP and H₂O solution onto a carbon plate (1.0 × 1.0 cm²). The reaction was electrolyzed at a constant potential of 1.0 V vs. Ag/AgCl for 3 h at room temperature. As shown in Table 1, benzylamine was almost fully oxidized (>99% conversion) and the selectivity of oxidative self-coupling product imine is of 94.9% (Table 1, entry 1). Electricity is indispensable for the oxidation reaction as the reaction was almost inactive when the voltage on working electrode was switched off (Table 1, entry 2). When molecular TEMPO-SO₃H was used as a homogeneous catalyst and carbon plate was used as working electrode, benzylamine was also almost fully oxidized (>99% conversion) under the otherwise identical conditions (Table 1, entry 3). However, the selectivity of self-coupling product is of only 61.3%, accompanying formation of large amount byproducts. These results demonstrate that suspending ion electrocatalyst TEMPO-SO₃⁻ in the cationic pores of TEMPO-SO₃@MIL-101(Cr)-HIM would significantly improve the product selectivity, controlled by the unique pore nature of the MOF. After the electrocatalytic reaction was proceeded for 1.5 h, the catalysis was deliberately interrupted. The TEMPO-SO₃@MIL-101(Cr)-HIM coated working electrode was subsequently immersed in acetonitrile to release the included guest molecules inside the pore space. GC analysis showed that the molecular ratio of released benzylamine reactant and *N*-benzylidenebenzylamine product is of 3.3, even though the conversion of benzylamine has been of 80%. This

result revealed that TEMPO-SO₃@MIL-101(Cr)-HIM exhibits preferred sorption capability of reactant over product molecules, which would selectively enrich substrate and release product molecules to improve the electrochemical selectivity by preventing formation of over-oxidized benzonitrile product. When MIL-101(Cr)-HIMBF₄ without TEMPO-SO₃⁻ anion inside the pore space was used instead of TEMPO-SO₃@MIL-101(Cr)-HIM under the otherwise identical conditions, benzylamine was almost not oxidized (Table 1, entry 4). This result indicates that the active sites are the suspended TEMPO-SO₃⁻ anions in the pores of TEMPO-SO₃@MIL-101(Cr)-HIM.

Table 1. Electrocatalytic properties of different electrocatalysts in oxidative self-coupling of benzylamine.^[a]

Entry	Electrocatalyst	Conv.(%)	Sel.(%) ^[b]
1	TEMPO-SO ₃ @MIL-101(Cr)-HIM	>99.9	94.9
2	TEMPO-SO ₃ @MIL-101(Cr)-HIM	trace	- ^[c]
3	TEMPO-SO ₃ H	>99.9	61.3
4	MIL-101(Cr)-HIMBF ₄	trace	-
5	TEMPO-SO ₃ H@MIL-101(Cr)	75.6	70.6
6	TEMPO@MIL-101(Cr)-HIMBF ₄	>99.9	80.8
7	TEMPO-COO@MIL-101(Cr)-HIM	89.6	80.7

[a] Reaction conditions: benzylamine (0.2 mmol), Bu₄NBF₄ acetonitrile solution (0.1 M, 4 mL), working electrode consisting of 0.0032 mmol TEMPO or TEMPO-SO₃⁻, Pt cathode, and Ag/AgCl reference electrode, room temperature, 3 h. [b] Yield and selectivity were determined by ¹H NMR in the presence of dibromomethane as an internal standard. The main side product is benzonitrile. [c] Switching off the working voltage.

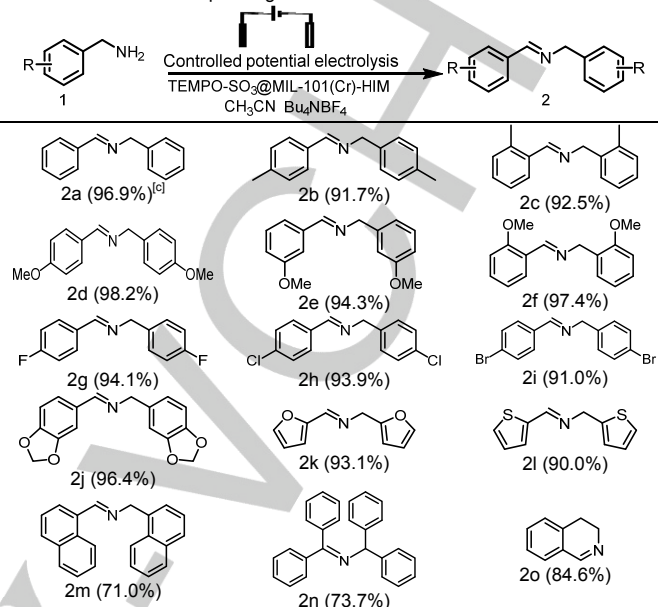
To make comparisons, we synthesized a series of control catalysts, including encapsulating TEMPO-SO₃H in neutral MIL-101(Cr) (denoted as TEMPO-SO₃H@MIL-101(Cr)), encapsulating neutral TEMPO in cationic MIL-101(Cr)-HIMBF₄ (denoted as TEMPO@MIL-101(Cr)-HIMBF₄) and encapsulating anionic TEMPO-COO⁻ in MIL-101(Cr)-HIM (denoted as TEMPO-COO@MIL-101(Cr)-HIM) (Figures S10-S16). As shown in Table 1 (entries 5-7), the catalytic properties of these control catalysts are much inferior to those of TEMPO-SO₃@MIL-101(Cr)-HIM. Because the interaction between electrocatalytic active moieties and pore matrices for TEMPO-SO₃H@MIL-101(Cr) and TEMPO@MIL-101(Cr)-HIMBF₄ is very weak, the active sites easily leach out of the pore space during catalysis. Because the carboxylate group of TEMPO-COO⁻ is easily coordinating to Cr^{III} metal nodes, the mobility of TEMPO-COO⁻ moieties in TEMPO-COO@MIL-101(Cr)-HIM is heavily confined, which are difficult to access to the working electrode. In addition, the electrical conductivity of neutral MIL-101(Cr) is much lower than that of ionic MIL-101(Cr)-HIM. These inferior characters of control

catalysts heavily deteriorated their electrocatalytic properties in the electroorganic reaction. In contrast, suspending anion electrocatalyst TEMPO-SO₃⁻ in the cationic pores of MIL-101(Cr)-HIM endows the active sites freely mobile and easy access to the working electrode surface, which is beneficial to polarize and activate reactant molecules. Combined with these superior characters, TEMPO-SO₃@MIL-101(Cr)-HIM exhibits high efficiency and selectivity in the electrocatalytic reaction.

Under the optimized electrocatalytic conditions, various substituted amines were investigated to expand the scope of the reaction substrates catalyzed by TEMPO-SO₃@MIL-101(Cr)-HIM. As shown in Table 2, the electronic properties of different substituents had little effect on substrate conversions and product selectivities with high product yields of 91.0–98.2% (Table 2, 2a–2l). Due to steric hindrance, the conversion of 1-naphthalenemethylamine is decreased with low imine product yield of 71.0% (2m). Similarly, diphenylmethylamine (2n) was obtained in low yield (73.7%), and the main side product is diphenylmethanone. Additionally, TEMPO-SO₃@MIL-101(Cr)-HIM is also highly efficient in dehydrogenation of secondary amines to form the corresponding imines, including 3,4-dihydroisoquinoline (2o, 84.6% yield) and (E)-N-benzylidene-1-phenylmethanamine (2a, 96.9%), under the identical electrocatalytic conditions.

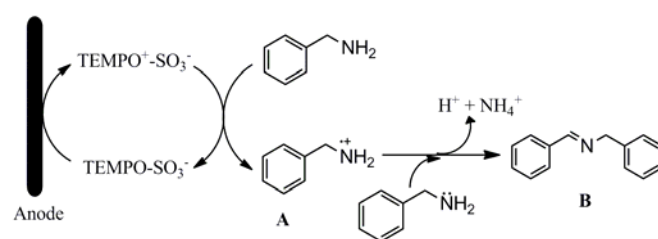
Immobilization of TEMPO-SO₃@MIL-101(Cr)-HIM on the surface of working electrode would simplify the work-up procedures and realize recycling usage of the electrocatalyst. Deferent to the active sites immobilized in traditional heterogeneous catalysts, the anionic TEMPO-SO₃⁻ active sites are suspended in the cationic pores of ionic MIL-101(Cr)-HIM, which are freely mobile. The heterogeneity and stability of the working electrode should be the most concerned issues, which would determine the long-term application capability of the working electrode. Recycling experiments showed that the working electrode is stable, which can be simply reused at least six runs in electrochemically oxidative coupling of benzylamine with basically retained catalytic properties (91.5% yield for the sixth run) (Figure S17). HPLC analysis of the digested working electrode showed that there is of 91.3% retained TEMPO-SO₃⁻ active sites inside the cationic pores of TEMPO-SO₃@MIL-101(Cr)-HIM. In contrast, the remained neutral TEMPO in TEMPO@MIL-101(Cr)-HIMBF₄ is of only 40.5% (Table S2). PXRD pattern of the reused working electrode is almost identical to that of as-synthesized one, which proved the structural stability of TEMPO-SO₃@MIL-101(Cr)-HIM in the electrocatalytic reaction (Figure S18). The above results indicate that suspending anion electrocatalyst TEMPO-SO₃⁻ in the cationic pores of MIL-101(Cr)-HIM would prevent leaching of active sites by strong electrostatic interaction during electrocatalysis. Compared with the corresponding homogeneous molecular catalyst, suspending TEMPO-SO₃⁻ in the cationic pores of the MOF immobilized on the working electrode would also prevent degradation of the oxidative intermediates (oxoammonium moieties) from TEMPO-SO₃⁻ on the counter electrode, and thus to improve the faradic efficiency, stability and catalytic efficiency.^[3,23]

Table 2. Electrochemically oxidative coupling of benzylamine and its derivatives to the corresponding imines.^[a,b]



[a] Reaction conditions: benzylamine (0.2 mmol), Bu₄NBF₄ acetonitrile solution (0.1 M, 4 mL), TEMPO-SO₃@MIL-101(Cr)-HIM carbon plate anode (consisting of 0.0032 mmol TEMPO-SO₃⁻), Pt cathode, and Ag/AgCl reference electrode, room temperature, 3 h. [b] Yield was determined by ¹H NMR in the presence of dibromomethane as an internal standard. [c] The yield was resulted from dehydrogenation of dibenzylamine.

On the basis of the results above, we proposed a plausible catalytic mechanism for the electrochemically oxidative self-coupling of benzylamine (Scheme 2).^[70–72] TEMPO-SO₃⁻ was firstly oxidized at the anode via a single electron transfer process to generate the corresponding active oxoammonium TEMPO⁺-SO₃⁻, which would oxidize benzylamine substrate to result in a radical-cation intermediate A. Intermediate A is highly reactive, which would easily react with another benzylamine molecule via oxidative dehydrogenation of the amine to afford benzylimine B, accompanying release of proton and ammonium cations. Meanwhile, active species TEMPO⁺-SO₃⁻ was reduced to TEMPO-SO₃⁻ via one electron transfer. At the cathode, H⁺ ions were electrochemically reduced to generate H₂ via electrochemical reduction.



Scheme 2. Proposed electrocatalytic cycles for oxidative coupling of benzylamine to form imine over TEMPO-SO₃@MIL-101(Cr)-HIM electrocatalyst.

Conclusions

We synthesized an imidazolium modified cationic MOF MIL-101(Cr)-HIMBr by post-modification, which exhibited high conductivity, compared with the pristine neutral MOF MIL-101(Cr). Anionic redox-active TEMPO-SO₃⁻ moieties were easily integrated and suspended inside the cationic pores of ionic MIL-101(Cr)-HIM by ion exchange, which served as an efficient electrocatalyst for oxidative self-coupling of benzylamines. Compared with the corresponding molecular catalyst, TEMPO-SO₃@MIL-101(Cr)-HIM exhibited superior electrocatalytic selectivity in the electrochemical reaction. This work highlights a general method for assembling suspended ion electrocatalysts with superior characters of high catalyst turnovers, conductivity, and electrochemical selectivity and stability. Because of the versatility and molecular tunability of ionic MOFs, we believe that the strategy reported in this work is generally applicable for design, synthesis and applications of heterogeneous electrocatalysts with distinct catalytic properties in electroorganic synthesis.

Experimental Section

Materials and Methods. All chemicals were obtained from commercial sources and were used without further purification. FT-IR spectra were collected from KBr pellets on an FTS-40 spectrophotometer. Powder X-ray diffraction (PXRD) data were recorded on a RIGAKU D/MAX 2550/PC for Cu K α radiation ($\lambda = 1.5406 \text{ \AA}$). Scanning electron microscopy (SEM) images were recorded on a Hitachi S-4800 equipment. Transmission electron microscopy (TEM) equipped with an energy dispersive X-ray (EDX) detector was recorded on a JEM 2100F equipment, and the samples were deposited onto ultrathin carbon films on carbon grids. ¹H NMR and ¹³C NMR spectra were recorded on a 400 MHz Bruker spectrometer and the chemical shifts were reported relative to internal standard TMS (0 ppm). A Micromeritics ASAP 2020 surface area analyzer was used to measure N₂ gas adsorption/desorption isotherms. The electrochemical measurements were conducted with a CHI 660E electrochemical workstation (Shanghai Chenhua, China) using a standard three-electrode system.

A typical procedure for preparation of TEMPO-SO₃@MIL-101(Cr)-HIM. MIL-101(Cr)-HIMBr was prepared according to previously reported procedures.^[61-65] 200 mg MIL-101(Cr)-HIMBr was added into 20 mL 1 M NaBF₄ aqueous solution, which was stirred at room temperature for 8 h, centrifuged, and washed with H₂O. This procedure was repeated five times. After Br⁻ was almost completely exchanged by BF₄⁻, the as-obtained solid was fully washed with H₂O to remove adsorbed NaBF₄, and dried at 100 °C for 12 h, affording MIL-101(Cr)-HIMBF₄. 29 mg (0.1 mmol) TEMPO-SO₃H and 2.4 mg (0.1 mmol) LiOH were dissolved in 10 mL MeOH, which was stirred at room temperature for 10 min. 100 mg MIL-101(Cr)-HIMBF₄ was added into the mixture, which was stirred at 60 °C for 12 h, then centrifuged and washed with H₂O. This procedure was repeated two times. The solid was collected by centrifugation, washed with MeOH, and dried at 60 °C under vacuum for 12 h, affording TEMPO-SO₃@MIL-101(Cr)-HIM.

A typical procedure for preparation of the working electrode. To prepare the catalyst ink, an as-prepared sample of TEMPO-SO₃@MIL-101(Cr)-HIM (20 mg) was ultrasonically dispersed in a mixture of 1.5% poly(vinylidene fluoride) (PVDF) NMP solution (0.25 mL) and H₂O (0.25

mL). 100 μ L of the resulting ink was pipetted onto a carbon plate (1.0 \times 1.0 cm²) as the working electrode. After air drying for 12 hours, the as-prepared electrode was further treated at 80 °C in an oven for 30 min before electrocatalysis.

Electrochemical measurements. Electrochemical measurements were conducted with a CHI 660E electrochemical workstation (Shanghai Chenhua, China) using a standard three-electrode system. To prepare the working electrode, an as-prepared sample (20 mg) was ultrasonically dispersed in a mixture of 1.5% PVDF NMP solution (0.25 mL) and H₂O (0.25 mL) for 15 min. 10 μ L of the resulting ink was pipetted onto a glassy carbon electrode (3 mm diameter). Cyclic voltammograms (CVs) were recorded in an electrolyte of Bu₄NBF₄ in CH₃CN (0.1 M, 10 mL) using the glassy carbon working electrode, a Pt wire auxiliary electrode and a Ag/AgCl (in 3 M KCl) reference electrode. Impedance spectra were collected using excitation amplitude of 5 mV within the frequency range spanning from 100 kHz to 0.01 Hz for the working electrode. Each measurement was performed at open-circuit potential in 0.1 M KCl aqueous solution (5 mL) containing 5 mM of [Fe(CN)₆]^{3-/4-} at room temperature. All impedance spectra were fitted to equivalent circuits using the ZView software.^[73] All measurements were collected at least in triplicate.

A typical procedure for electrocatalytic oxidation of benzylamine. A mixture of benzylamine (0.2 mmol) in 0.1 M Bu₄NBF₄ acetonitrile solution (4 mL) was added into an undivided cell. The cell was equipped with the as-prepared working electrode as anode, Pt plate as cathode and Ag/AgCl (in 3 M KCl) as reference electrode. The reaction mixture was stirred and electrolyzed at a constant potential of 1.0 V at room temperature for 3 h. When the electrocatalytic reaction was finished, the solution was extracted with EtOAc (3 \times 10 mL). The combined organic layer was dried over Na₂SO₄, and filtered. The solvent was removed with a rotary evaporator. The yield was determined by ¹H NMR in the presence of dibromomethane as an internal standard.

Acknowledgements

We are grateful for the financial support of the National Natural Science Foundation of China (grant nos. 21373180, 21525312 and 21872122).

Keywords: Conductivity • Electrocatalysis • Metal-organic frameworks • Electroselectivity • Suspended ion catalysts

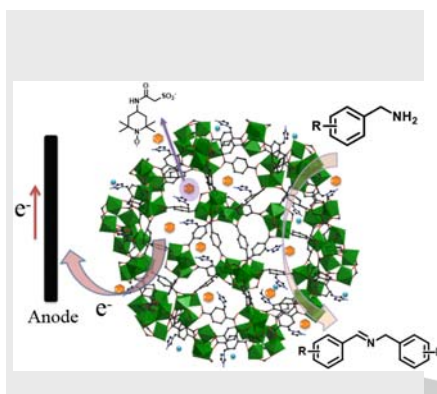
- [1] E. J. Horn, B. R. Rosen, P. S. Baran, *ACS Cent. Sci.* **2016**, *2*, 302-308.
- [2] Y. Mo, K. F. Jensen, *Chem. Eur. J.* **2018**, *24*, 10260-10265.
- [3] A. Das, S. S. Stahl, *Angew. Chem. Int. Ed.* **2017**, *56*, 8892-8897.
- [4] X. Yi, X. Hu, *Angew. Chem. Int. Ed.* **2019**, *58*, 4700-4704.
- [5] L. Schulz, M. Enders, B. Elsler, D. Schollmeyer, K. M. Dyballa, R. Franke, S. R. Waldvogel, *Angew. Chem. Int. Ed.* **2017**, *56*, 4877-4881.
- [6] Z.-J. Wu, H.-C. Xu, *Angew. Chem. Int. Ed.* **2017**, *56*, 4734-4738.
- [7] C. Li, Y. Kawamata, H. Nakamura, J. C. Vantourout, Z. Liu, Q. Hou, D. Bao, J. T. Starr, J. Chen, M. Yan, P. S. Baran, *Angew. Chem. Int. Ed.* **2017**, *56*, 13088-13093.
- [8] H.-B. Zhao, Z.-J. Liu, J. Song, H.-C. Xu, *Angew. Chem. Int. Ed.* **2017**, *56*, 12732-12735.
- [9] N. Sauermann, T. H. Meyer, C. Tian, L. Ackermann, *J. Am. Chem. Soc.* **2017**, *139*, 18452-18455.
- [10] Y. Ashikari, T. Nokami, J. Yoshida, *J. Am. Chem. Soc.* **2011**, *133*, 11840-11843.

- [11] E. J. Horn, B. R. Rosen, Y. Chen, J. Tang, K. Chen, M. D. Eastgate, P. S. Baran, *Nature* **2016**, *533*, 77-81.
- [12] A. Gitkis, J. Y. Becker, *Electrochim. Acta* **2010**, *55*, 5854-5859.
- [13] P. Wang, S. Tang, P. Huang, A. Lei, *Angew. Chem. Int. Ed.* **2017**, *56*, 3009-3013.
- [14] Y.-Y. Jiang, S. Liang, C.-C. Zeng, L.-M. Hu, B.-G. Sun, *Green Chem.* **2016**, *18*, 6311-6319.
- [15] O. Baslé, N. Borduas, P. Dubois, J. M. Chapuzet, T.-H. Chan, J. Lessard, C.-J. Li, *Chem. Eur. J.* **2010**, *16*, 8162-8166.
- [16] T. Sawamura, K. Takahashi, S. Inagi, T. Fuchigami, *Angew. Chem. Int. Ed.* **2012**, *51*, 4413-4416.
- [17] F. Kakiuchi, T. Kochi, H. Mutsutani, N. Kobayashi, S. Urano, M. Sato, S. Nishiyama, T. Tanabe, *J. Am. Chem. Soc.* **2009**, *131*, 11310-11311.
- [18] S. Mukherjee, D. A. Cullen, S. Karakalos, K. Liu, H. Zhang, S. Zhao, H. Xu, K. L. More, G. Wang, G. Wu, *Nano Energy* **2018**, *48*, 217-226.
- [19] H. Tao, C. Choi, L.-X. Ding, Z. Jiang, Z. Han, M. Jia, Q. Fan, Y. Gao, H. Wang, A. W. Robertson, S. Hong, Y. Jung, S. Liu, Z. Sun, *Chem* **2019**, *5*, 204-214.
- [20] J. Zheng, Y. Lyu, M. Qiao, R. Wang, Y. Zhou, H. Li, C. Chen, Y. Li, H. Zhou, S. P. Jiang, S. Wang, *Chem* **2019**, *5*, 617-633.
- [21] Q. Lu, F. Jiao, *Nano Energy* **2016**, *29*, 439-456.
- [22] Z. Sun, T. Ma, H. Tao, Q. Fan, B. Han, *Chem* **2017**, *3*, 560-587.
- [23] L. Yang, L. Cao, R. Huang, Z.-W. Hou, X.-Y. Qian, B. An, H.-C. Xu, W. Lin, C. Wang, *ACS Appl. Mater. Interfaces* **2018**, *10*, 36290-36296.
- [24] H.-C. Zhou, S. Kitagawa, *Chem. Soc. Rev.* **2014**, *43*, 5415-5418.
- [25] H. Furukawa, K. E. Cordova, M. O'Keeffe, O. M. Yaghi, *Science* **2013**, *341*, 1230444.
- [26] G. Maurin, C. Serre, A. Cooper, G. Férey, *Chem. Soc. Rev.* **2017**, *46*, 3104-3107.
- [27] T. Islamoglu, S. Goswami, Z. Li, A. J. Howarth, O. K. Farha, J. T. Hupp, *Acc. Chem. Res.* **2017**, *50*, 805-813.
- [28] B. Li, H.-M. Wen, Y. Cui, W. Zhou, G. Qian, B. Chen, *Adv. Mater.* **2016**, *28*, 8819-8860.
- [29] W. P. Lustig, S. Mukherjee, N. D. Rudd, A. V. Desai, J. Li, S. K. Ghosh, *Chem. Soc. Rev.* **2017**, *46*, 3242-3285.
- [30] Q.-L. Zhu, Q. Xu, *Chem. Soc. Rev.* **2014**, *43*, 5468-5512.
- [31] Q.-G. Zhai, X. Bu, X. Zhao, D.-S. Li, P. Feng, *Acc. Chem. Res.* **2017**, *50*, 407-417.
- [32] T. Zhang, W. Lin, *Chem. Soc. Rev.* **2014**, *43*, 5982-5993.
- [33] J. Liu, L. Chen, H. Cui, J. Zhang, L. Zhang, C.-Y. Su, *Chem. Soc. Rev.* **2014**, *43*, 6011-6061.
- [34] S. M. J. Rogge, A. Bavykina, J. Hajek, H. Garcia, A. I. Olivos-Suarez, A. Sepúlveda-Escribano, A. Vimont, G. Clet, P. Bazin, F. Kapteijn, M. Daturi, E. V. Ramos-Fernandez, F. X. Llabrés i Xamena, V. Van Speybroeck, J. Gascon, *Chem. Soc. Rev.* **2017**, *46*, 3134-3184.
- [35] X. Lian, Y. Fang, E. Joseph, Q. Wang, J. Li, S. Banerjee, C. Lollar, X. Wang, H.-C. Zhou, *Chem. Soc. Rev.* **2017**, *46*, 3386-3401.
- [36] W.-Y. Gao, M. Chrzanowski, S. Ma, *Chem. Soc. Rev.* **2014**, *43*, 5841-5866.
- [37] A. H. Chughtai, N. Ahmad, H. A. Younus, A. Laypkov, F. Verpoort, *Chem. Soc. Rev.* **2015**, *44*, 6804-6849.
- [38] H. R. Moon, D.-W. Lim, M. P. Suh, *Chem. Soc. Rev.* **2013**, *42*, 1807-1824.
- [39] M. Yoon, R. Srirambalaji, K. Kim, *Chem. Rev.* **2012**, *112*, 1196-1231.
- [40] A. Dhakshinamoorthy, H. Garcia, *Chem. Soc. Rev.* **2014**, *43*, 5750-5765.
- [41] M. Zhao, S. Ou, C.-D. Wu, *Acc. Chem. Res.* **2014**, *47*, 1199-1207.
- [42] C. Wang, D. Liu, W. Lin, *J. Am. Chem. Soc.* **2013**, *135*, 13222-13234.
- [43] L. Jiao, Y. Wang, H.-L. Jiang, Q. Xu, *Adv. Mater.* **2018**, *30*, 1703663.
- [44] L. Li, J. He, Y. Wang, X. Lv, X. Gu, P. Dai, D. Liu, X. Zhao, *J. Mater. Chem. A* **2019**, *7*, 1964-1988.
- [45] P. M. Usov, B. Huffman, C. C. Epley, M. C. Kessinger, J. Zhu, W. A. Maza, A. J. Morris, *ACS Appl. Mater. Interfaces* **2017**, *9*, 33539-33543.
- [46] X. Sun, K.-H. Wu, R. Sakamoto, T. Kusamoto, H. Maeda, X. Ni, W. Jiang, F. Liu, S. Sasaki, H. Masunaga, H. Nishihara, *Chem. Sci.* **2017**, *8*, 8078-8085.
- [47] B. Nohra, H. E. Moll, L. M. R. Albelo, P. Mialane, J. Marrot, C. Mellot-Draznieks, M. O'Keeffe, R. N. Biboum, J. Lemaire, B. Keita, L. Nadjio, A. Dolbecq, *J. Am. Chem. Soc.* **2011**, *133*, 13363-13374.
- [48] C. Zhao, X. Dai, T. Yao, W. Chen, X. Wang, J. Wang, J. Yang, S. Wei, Y. Wu, Y. Li, *J. Am. Chem. Soc.* **2017**, *139*, 8078-8081.
- [49] N. Kornienko, Y. Zhao, C. S. Kley, C. Zhu, D. Kim, S. Lin, C. J. Chang, O. M. Yaghi, P. Yang, *J. Am. Chem. Soc.* **2015**, *137*, 14129-14135.
- [50] L. Yang, S. Kinoshita, T. Yamada, S. Kanda, H. Kitagawa, M. Tokunaga, T. Ishimoto, T. Ogura, R. Nagumo, A. Miyamoto, M. Koyama, *Angew. Chem. Int. Ed.* **2010**, *49*, 5348-5351.
- [51] G. Givaja, P. Amo-Ochoa, C. J. Gómez-García, F. Zamora, *Chem. Soc. Rev.* **2012**, *41*, 115-147.
- [52] L. Sun, M. G. Campbell, M. Dincă, *Angew. Chem. Int. Ed.* **2016**, *55*, 3566-3579.
- [53] X. Huang, P. Sheng, Z. Tu, F. Zhang, J. Wang, H. Geng, Y. Zou, C.-A. Di, Y. Yi, Y. Sun, W. Xu, D. Zhu, *Nat. Commun.* **2015**, *6*, 7408.
- [54] M. H. Hassan, R. R. Haikal, T. Hashem, J. Rinck, F. Koeniger, P. Thissen, S. Heißler, C. Wöll, M. H. Alkordi, *ACS Appl. Mater. Interfaces* **2019**, *11*, 6442-6447.
- [55] J. Cui, Z. Xu, *Chem. Commun.* **2014**, *50*, 3986-3988.
- [56] L. S. Xie, L. Sun, R. Wan, S. S. Park, J. A. DeGayner, C. H. Hendon, M. Dincă, *J. Am. Chem. Soc.* **2018**, *140*, 7411-7414.
- [57] M. Watanabe, M. L. Thomas, S. Zhang, K. Ueno, T. Yasuda, K. Dokko, *Chem. Rev.* **2017**, *117*, 7190-7239.
- [58] K. Fujie, H. Kitagawa, *Coord. Chem. Rev.* **2016**, *307*, 382-390.
- [59] W.-L. He, X.-L. Yang, M. Zhao, C.-D. Wu, *J. Catal.* **2018**, *358*, 43-49.
- [60] W.-L. He, M. Zhao, C.-D. Wu, *Angew. Chem. Int. Ed.* **2019**, *58*, 168-172.
- [61] G. Férey, C. Mellot-Draznieks, C. Serre, F. Millange, J. Dutour, S. Surble, I. Margiolaki, *Science* **2005**, *309*, 2040-2042.
- [62] D. Liu, G. Li, H. O. Liu, *Appl. Surf. Sci.* **2018**, *428*, 218-225.
- [63] M. G. Goesten, K. B. Sai Sankar Gupta, E. V. Ramos-Fernandez, H. Khajavi, J. Gascon, F. Kapteijn, *CrystEngComm* **2012**, *14*, 4109-4111.
- [64] M. L. Linares, N. Sánchez, R. Alajarin, J. J. Vaquero, J. Alvarez-Builla, *Synthesis* **2001**, *3*, 382-388.
- [65] F. Zadehmadi, S. Tangestaninejad, M. Moghadam, V. Mirkhani, I. Mohammadpoor-Baltork, A. R. Khosropour, R. Kardanpour, *J. Solid State Chem.* **2014**, *218*, 56-63.
- [66] V. Zima, D. S. Patil, D. S. Raja, T.-G. Chang, C.-H. Lin, K. Shimakawa, T. Wagner, *J. Solid State Chem.* **2014**, *217*, 150-158.
- [67] S. Carvalho, L. Palermo, L. Boak, K. Sorbie, E. F. Lucas, *Energy Fuels* **2017**, *31*, 10648-10654.
- [68] S. Kobayashi, Y. Mori, J. S. Fossey, M. M. Salter, *Chem. Rev.* **2011**, *111*, 2626-2704.
- [69] K. C. Nicolaou, C. J. N. Mathison, T. Montagnon, *Angew. Chem. Int. Ed.* **2003**, *42*, 4077-4082.
- [70] Y. Wu, H. Yi, A. Lei, *ACS Catal.* **2018**, *8*, 1192-1196.
- [71] H. Huang, J. Huang, Y.-M. Liu, H.-Y. He, Y. Cao, K.-N. Fan, *Green Chem.* **2012**, *14*, 930-934.
- [72] X. Cui, Y. Li, S. Bachmann, M. Scalone, A.-E. Surkus, K. Junge, C. Topf, M. Beller, *J. Am. Chem. Soc.* **2015**, *137*, 10652-10658.
- [73] S. S. Zhang, K. Xu, T. R. Jow, *Electrochim. Acta* **2004**, *49*, 1057-1061.

Entry for the Table of Contents

FULL PAPER

Suspending ion electrocatalysts in charged metal-organic frameworks (MOFs) markedly improves the conductivity and catalytic efficiency, and catalytic selectivity in electroorganic synthesis, compared with the corresponding neutral MOFs and homogeneous molecular catalysts, respectively.



Wei-Wei Guo, Chi Zhang, Ji-Jie Ye, Zi-Kun Liu, Kai Chen, Chuan-De Wu*

Page No. – Page No.

Suspending Ion Electrocatalysts in Charged Metal-Organic Frameworks to Improve the Conductivity and Selectivity in Electroorganic Synthesis